




Anti-disturbance composite tracking control for a coupled two-tank MIMO process with experimental studies

Houssemeddine Gouta , Waseem Haysam Al-Ashek and Basem Saad

Department of Electrical and Electronics Engineering, British Applied College, Umm Al Quwain, United Arab Emirates

ABSTRACT

Coupled multiple-tank systems are very important for a wide range of industrial applications due to their unique uses. However, the liquid level control for the coupled two-tank multi-input multi-output (MIMO) system is quite challenging because it has strong nonlinearity and coupling, and it is susceptible to multiple external disturbances. For this process, this paper proposes a novel anti-disturbance control strategy consisting on a nonlinear composite hierarchical anti-disturbance predictive control (CHADPC). First, a model-based explicit nonlinear model predictive controller (ENMPC) is designed assuming that all disturbances are measurable and its global exponential stability is proved. Then, a nonlinear disturbance observer (DO) is designed to estimate the lumped disturbances. The composite controller handling the estimated disturbances is then proposed. Finally, simulation and experimental tracking control tests under perturbations and comparisons with recently reported works have been carried out to highlight the promising performance of the proposed ENMPC and CHADPC schemes.

ARTICLE HISTORY

Received 29 June 2021
Accepted 25 March 2022

KEYWORDS

Model predictive control;
real-time control;
exponential stability;
disturbance observer;
comparative study;
experimental validation

1. Introduction

Often, industrial applications involve multiple interconnected tanks, such as in wastewater treatment and biomedical facilities. Some of their liquid levels may be controlled to maintain a constant, while others must follow a time-varying level profile [1,2]. In a waste water treatment plant, anaerobic digestion of high strength waste water slurries results in the formation of biogas, which is used to produce green energy by converting heat and power from the biogas. Sludge remaining from this process is rich in nutrients and can be used in agriculture. In this process, pre-treatment tanks, primary tanks, aeration tanks, secondary tanks, and multiple digestion tanks are interconnected. To reach a high performance in such a process, independent level control (levels may differ according to production) is essential [1]. A similar situation also exists in the sewage treatment of pulp and paper mills [2].

Similarly, an automated drug dispensing system may control systemic arterial pressure (AP), cardiac output (CO), and left atrial pressure (PLA) simultaneously, and these parameters have sensitive correlations between them similar to interconnected tanks. AP, CO, and PLA must have their independent benchmarks maintained by controlling the injection of drugs through multiple inputs [3]. Controllers have to perform both tasks i.e., make one process variable follow the time-varying reference signal while keeping the other process variable constant. In general, controllers

of the proportional–integral–derivative (PID) family together with a feed-forward controller are well suited for such a requirement which was recently shown in [4] and [5]. However, the main drawback of this type of controllers is that they first require the linearization of the nonlinear system model, which is difficult for complex systems.

This paper is motivated by [4], which proposes a Fractional-order PI controller for the coupled two-tank MIMO system illustrated in Figure 1. Nevertheless, this paper adopts, for this liquid level system (see [6]), the model predictive control (MPC) strategy, which shows recent promising results in a comparative study in [7] and in the adaptive control in [8]. As a practical alternative approach, MPC has received much attention and has been considered by many researchers as one of the most promising methods in control engineering [9,10]. Moreover, it is worth noticing that MPC's model-based control strategy highly relies on predicting the performance of the plant [11]. As a result, the main limitations of MPC are the limited accuracy of its predictive model and the low efficiency of its control strategy. Thus, an optimal control decision can be made based on optimization according to this prediction [12]. This predictive property of MPC makes it a suitable control strategy for complex and nonlinear level systems. Specifically for the reference tracking problem, MPC can take into account the future value of the given reference trajectory to improve the performance in the

CONTACT Houssemeddine Gouta  gouta.houssemeddine@gmail.com  Department of Electrical and Electronics Engineering, British Applied College, Al Humrah B, Umm Al Quwain, United Arab Emirates

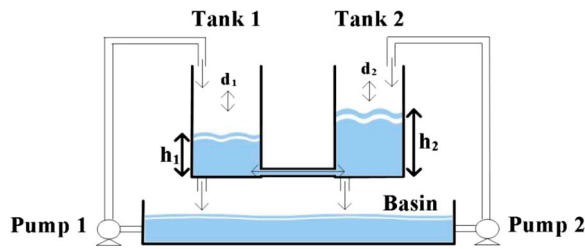


Figure 1. Coupled two-tank MIMO system.

sense that not only the current tracking error can be suppressed, but also all future errors. ENMPC represents the continuous-time solution of the nonlinear MPC approach, which generally requires the solution of an optimization problem at each sampling instance. This is an obstacle for real-time implementation due to the high computational cost. An analytical solution of the nonlinear MPC can be found by approximating the tracking error and the control effort in a receding horizon using their Taylor expansion up to a certain order, and consequently, the closed-form control law can be explicitly formulated without online optimization [12].

On the other hand, it is worth noticing that disturbances are common in most industrial systems and have negative effects on the performance and even the stability of control systems [13]. Therefore, the problem of disturbance attenuation or suppression remains a hot topic in the field of control. When the disturbances are well estimated and provided, the control system can explicitly consider them and compensate for them. Based on a nonlinear DO, this basic idea of composite hierarchical anti-disturbance control was first proposed in [14] for a system subject to external disturbances and model uncertainties. The basic controller may not only be designed for achieving tracking performance, but also for disturbance attenuation, such as H_∞ or stochastic control theory [15]. Several research works have been done where the disturbances are estimated and the opposite of their estimation is used in control. Some interesting methods in this field are the disturbance observer presented in [16], two-time-scale based observation in [17] and the DO using neural network technique in [18]. Some recent promising applications of the disturbance observers on experimental setups abound in literature such as [18–20]. In addition, other promising results of the application of the active disturbance rejection control technique as recently shown in [21–25]. This paper revisits [26] and adopts the slow time-varying DO introduced in [16]. The novelties of the proposed work are as given below:

- (i) CHADPC method has not been used before for the level control problem of coupled two-tank MIMO system as per the best of the knowledge of the authors.

- (ii) A design methodology is presented, minimizing the receding horizon performance index, to find the ENMPC ensuring an exponential stability. This design methodology is an extension of the two recent works in [6] and [7].
- (iii) Experimental comparisons between ENMPC and CHADPC presented, by validation on a two-tank system, to show that CHADPC method performs better.
- (iv) Brief comparisons of benchmark tracking performance and disturbance rejection capabilities with other recent reported works are presented to show that the performance of the proposed CHADPC method is better than that of several other existing level controllers.

The rest of the sections are described as follows: Section 2 describes the system modelling and the problem formulation, while Section 3 contains the proposed ENMPC design and its stability study. Section 4 presents the DO and the CHADPC method. The simulation and experimental results of the ENMPC and CHADPC strategies are presented and discussed in Section 5, while conclusions are given in Section 6.

The main objectives of this paper are as below:

- (i) To design an ENMPC for a particular class of nonlinear systems, to which the coupled two-tank MIMO system belongs, and address its exponential stability.
- (ii) To design a CHADPC by developing an interconnected DO to the designed ENMPC for the same class of MIMO systems under slow time-varying disturbances.
- (iii) To validate the two control schemes on an experimental setup.
- (iv) To compare experimentally the CHADPC method with the ENMPC one.
- (v) To compare the level control performance of the present work with those reported in earlier similar studies.

2. Problem formulation

Figure 1 shows a schematic diagram of a state-coupled two-tank MIMO system with two degrees of freedom. This system consists of a fluid basin, two pumps, two tanks of equal area with openings, and level sensors at the bottom of each tank. In this experimental setup, Pump 1 and Pump 2, respectively supply inflow to tanks 1 and 2 and the common outflow from tank i becomes the inflow for Tank j , $i, j = 1, 2$ and vice versa. The other outflows from tanks 1 and 2 are discharged to the basin. In terms of the system dynamic model, the following features are first introduced:

- (i) Pump 1 and Pump 2 are identical.

Table 1. Numerical values of system parameters.

Parameter	Symbol	Numerical value
Each tank area	A	225cm ²
Orifices sectional area	a	0.7854cm ²
Common orifice sectional area	a_{12}	0.9143cm ²
Pumps constant	K_p	3.4717 cm ³ /(V.s)
Gravitational constant	g	981 cm/s ²

- (ii) $u = [u_1 \ u_2]^T$, where u_1 and u_2 are the voltages applied respectively at the input terminals of the two pumps (both are bounded by 0 and 12 volts), represents the input of the electromechanical system.
- (iii) the liquid levels h_1 and h_2 are always greater than 1 cm and less than 30 cm.
- (iv) $y = [h_1 \ h_2]^T$ represents the output of the system.

Considering the liquid level system modelling in [6], the following dynamic equations for the system are given as:

$$\begin{cases} \dot{h}_1(t) = -c_1\sqrt{h_1(t)} - c_{12}\text{sign}(h_1(t) \\ \quad -h_2(t))\sqrt{|h_1(t) - h_2(t)|} + c_2u_1(t) \\ \dot{h}_2(t) = -c_1\sqrt{h_2(t)} - c_{12}\text{sign}(h_2(t) \\ \quad -h_1(t))\sqrt{|h_2(t) - h_1(t)|} + c_2u_2(t) \end{cases} \quad (1)$$

where parameters $c_1 = \frac{a}{A}\sqrt{2g}$, $c_2 = \frac{K_p}{A}$ and $c_{12} = \frac{a_{12}}{A}\sqrt{2g}$ are given in Table 1.

Remark 2.1: Although dynamics (1) is a generic model, it can be used to present liquid levels depending on some external disturbances. In fact, the liquid level dynamic used in this paper is altered by taking into account additional elements that operate as disturbances. The long distance between each pump and its associated tank as well as the pump faults, such as missing vanes or deposition of some residues in the impeller, cause a liquid arrival delay every time when the control signal is changed. As a result, the level h_i is subject to a small drop, which is undesirable. Furthermore, due to the unexpected accumulation of residues in some pipelines or valve faults, the level h_i may experience a fast increase. These two events cause the level to drop and rise somewhat. They are treated as lumped disturbances in the controlled liquid level system in this study. These phenomena can occur in a variety of industrial operations, such as wastewater treatment.

In this paper, we assume that the two sensors are present to measure the liquid levels in the two tanks. Considering the saturation of the inputs, the objective is to design a disturbance observer-based control scheme to control the liquid levels h_1 and h_2 with respect to two desired set points r_1 and r_2 , respectively. Considering Remark 2.1, the mathematical model of the considered

system under disturbances can be written as follows:

$$\begin{cases} \dot{h} = f(h) + g(h)u + d \\ y = h \end{cases} \quad (2)$$

where $h = [h_1 \ h_2]^T$ is the internal state of the system ($h \in \mathcal{H} \subset \mathfrak{R}^2$), $f(h) = [f_1(h) \ f_2(h)]^T \in \mathfrak{R}^2$ with:

$$f_i(h) = -c_1\sqrt{h_i} - c_{12}\text{sign}(h_i - h_j)\sqrt{|h_i - h_j|}, i = 1, 2 \quad (3)$$

$u = [u_1 \ u_2]^T \in \mathcal{U} \subset \mathfrak{R}^2$ the control input, $y \in \mathfrak{R}^2$ the measured output, $g(h)$ is a matrix in $\mathfrak{R}^{2 \times 2}$ and $d = [d_1 \ d_2]^T$ represents the lumped disturbances acting on the liquid levels h_1 and h_2 .

3. Explicit nonlinear MPC design

In MPC theory, the concept of moving horizon control can be explained as designing a state trajectory $\hat{h}(t + \tau)$ at any time t within a moving time frame located at time t with respect to $h(t)$ as an initial condition, which is controlled by a control signal $\hat{u}(t + \tau)$ together with the associated prediction $\hat{y}(t + \tau)$. The tracking control can be achieved by minimizing a receding horizon performance index $\mathcal{J} \in \mathfrak{R}$ for a receding horizon given by:

$$\mathcal{J} = \frac{1}{2} \int_0^{T_p} (\hat{y}(t + \tau) - \hat{r}(t + \tau))^T (\hat{y}(t + \tau) - \hat{r}(t + \tau)) d\tau \quad (4)$$

where T_p is the predictive period.

The conventional MPC algorithm requires the solution of a working point at each sampling instance to obtain the control signals. To avoid the resulting intensive online computation, it is necessary to assume an explicit solution for the nonlinear MPC problem based on the approximation of the tracking error in the receding prediction horizon [12]. In this paper, the following assumptions are made for the nonlinear system (2):

A1: The zero-point dynamics are stable [27].

A2: Each of the outputs $y(t)$ has the same relative degree ρ [27].

A3: The output $y(t)$ and the reference $r(t)$ are sufficiently often continuously differentiable with respect to t .

Since assumptions A1, A2 and A3 are satisfied in our studied system, the nonlinear model (2) is extended by Taylor-series expansion to its relative degree ρ as follows:

$$\begin{cases} \hat{y}(t + \tau) \doteq \bar{T}(\tau)\bar{Y}(t) \\ \hat{r}(t + \tau) \doteq \bar{T}(\tau)\bar{R}(t) \end{cases} \quad (5)$$

where $\bar{T}(\tau) = [I_2 \quad \tau I_2]$ with $I_2 = \begin{bmatrix} 1 & 0 \\ 0 & 1 \end{bmatrix}$, $\bar{Y}(t) = [y(t) \quad \dot{y}(t)]^T = [y_1(t) \quad y_2(t) \quad \dot{y}_1(t) \quad \dot{y}_2(t)]^T$ and $\bar{R}(t) = [r(t) \quad \dot{r}(t)]^T = [r_1(t) \quad r_2(t) \quad \dot{r}_1(t) \quad \dot{r}_2(t)]^T$.

Recalling Equation (4) and the output and reference approximation (5), we can write the receding horizon performance index \mathcal{J} in matrix form as:

$$\mathcal{J} = \frac{1}{2}(\bar{Y}(t) - \bar{R}(t))^T \mathcal{T}(T_p)(\bar{Y}(t) - \bar{R}(t)) \quad (6)$$

where $\mathcal{T}(T_p) = \int_0^{T_p} \bar{T}^T(\tau) \bar{T}(\tau) d\tau = \begin{bmatrix} \mathcal{T}_{(1,1)} & \mathcal{T}_{(1,2)} \\ \mathcal{T}_{(2,1)} & \mathcal{T}_{(2,2)} \end{bmatrix}$

with $\mathcal{T}_{(i,j)} = \frac{T_p^{i+j-1}}{(i+j-1)(i-1)!(j-1)!} I_2$. The time derivative of the reference and the output vectors gives:

$$\begin{cases} \dot{r} = f(r) + g(r)\tilde{u}_d + d \\ \dot{y} = \dot{h} = f(h) + g(h)\tilde{u} + d \end{cases} \quad (7)$$

where \tilde{u}_d is the desired control input. Let:

$$\bar{Y}(t) - \bar{R}(t) = \mathcal{M}(h, r) + \begin{bmatrix} 0_{2 \times 1} \\ \mathcal{H}(h, \tilde{u}) \end{bmatrix} \quad (8)$$

where $\mathcal{M}(h, r) = \begin{bmatrix} e_h \\ \Delta f - g(r)\tilde{u}_d \end{bmatrix}$, $0_{2 \times 1} = \begin{bmatrix} 0 \\ 0 \end{bmatrix}$, $e_h = \begin{bmatrix} h_1 - r_1 \\ h_2 - r_2 \end{bmatrix}$, $\Delta f = \begin{bmatrix} f_1(h) - f_1(r) \\ f_2(h) - f_2(r) \end{bmatrix}$ and $\mathcal{H}(h, \tilde{u}) = g(h)\tilde{u}$. By invoking (6) and (8), we obtain:

$$\mathcal{J} = \frac{1}{2}(\mathcal{M}^T \mathcal{T}(T_p) \mathcal{M} + \mathcal{T}_{\{2,2\}} \mathcal{H}^T \mathcal{H} + 2\mathcal{M}^T \bar{\mathcal{T}}_2 \mathcal{H}) \quad (9)$$

where $\bar{\mathcal{T}}_2 = \begin{bmatrix} \frac{T_p^2}{2} I_2 & \frac{T_p^3}{3} I_2 \end{bmatrix}^T$ is the sub-matrix composed of the 3rd and 4th columns and $\mathcal{T}_{\{2,2\}} = \frac{T_p^3}{3} I_2$ is the (2, 2)th sub-matrix of matrix $\mathcal{T}(T_p)$. By solving the following Eq. (10) which is given by:

$$\frac{\partial \mathcal{J}}{\partial \tilde{u}} = \frac{1}{2}(2\mathcal{M}^T \bar{\mathcal{T}}_2 g(h) + 2\tilde{u}^T g(h)^T g(h) \mathcal{T}_{\{2,2\}}) = 0_{1 \times 2} \quad (10)$$

we obtain an explicit solution of predictive control as:

$$\tilde{u} = \begin{bmatrix} \tilde{u}_1 \\ \tilde{u}_2 \end{bmatrix} = g(h)^{-1}(-\mathcal{T}_{\{2,2\}}^{-1} \bar{\mathcal{T}}_2^T \mathcal{M}) \quad (11)$$

Finally, by invoking (7) and (11), an ENMPC law can be given by the following expression:

$$\tilde{u} = -g(h)^{-1}(ke_h - f(h) - \dot{r} + d) \quad (12)$$

where $k = \frac{3}{2T_p}$.

Proposition 3.1: Consider the system under disturbances given by (2) and let $r = [r_1 \quad r_2]^T \in \mathfrak{R}^2$ be a reference trajectories vector with bounded time derivative, hence the control law (12) makes $y = r$ a globally exponentially stable equilibrium.

Proof: Let $e_h = h - r$ the tracking error for the model (2). Hence, its time derivative can be written as follows:

$$\dot{e}_h = \Delta f + g(h)\tilde{u} - g(r)\tilde{u}_d \quad (13)$$

By invoking (7) and (13), we obtain:

$$\dot{e}_h = A_e e_h + 2f(h) \quad (14)$$

where $A_e = \begin{bmatrix} -k & 0 \\ 0 & -k \end{bmatrix}$ and $f(h)$ is defined in (2). The characteristic polynomial of the matrix A_e is:

$$s^2 + 2ks + k^2 = 0 \quad (15)$$

where s is Laplace operator. Then, by applying the Routh stability criterion, $k > 0$ guarantees that matrix A_e is Hurwitz. Let the scalar $\nu = e_h^T \mathcal{P} e_h$, with \mathcal{P} a positive definite matrix. Then its time derivative is:

$$\dot{\nu} = e_h^T (A_e^T \mathcal{P} + \mathcal{P} A_e) e_h + 4e_h^T \mathcal{P} f(h) \quad (16)$$

Since matrix A_e is Hurwitz, one can find a 2×2 positive definite matrix \mathcal{Q} which satisfies:

$$A_e^T \mathcal{P} + \mathcal{P} A_e = -\mathcal{Q} \quad (17)$$

so:

$$\dot{\nu} \leq -e_h^T \mathcal{Q} e_h + 4 \|e_h^T \mathcal{P} f(h)\| \quad (18)$$

Assuming that $f(h)$ is differentiable, its time derivative is also bounded. Hence, $\|f_1(h)\| \leq \delta_1 \|e_h\|$ and $\|f_2(h)\| \leq \delta_2 \|e_h\|$. Such that $f(h) = \begin{bmatrix} f_1(h) \\ f_2(h) \end{bmatrix}$, we can write $\|f(h)\| \leq \delta \|e_h\|$, where $\delta = \sqrt{\delta_1^2 + \delta_2^2}$. The Rayleigh inequalities are then, obtained as:

$$\begin{cases} -\alpha_m(\mathcal{Q}) \|e_h\|^2 \leq -e_h^T \mathcal{Q} e_h \leq -\alpha_m(\mathcal{Q}) \|e_h\|^2 \\ \alpha_m(\mathcal{P}) \|e_h\|^2 \leq \nu \leq \alpha_M(\mathcal{P}) \|e_h\|^2 \end{cases} \quad (19)$$

with $\alpha_m(\mathcal{Q})$ and $\alpha_M(\mathcal{P})$ are, respectively, the minimum eigenvalue of \mathcal{Q} and the maximum eigenvalue of \mathcal{P} . Using Cauchy-Schwartz inequality, we can write:

$$\dot{\nu} \leq (2\alpha_M(\mathcal{P})\delta - \alpha_m(\mathcal{Q})) \|e_h\|^2 \quad (20)$$

Hence, we obtain:

$$\dot{\nu} \leq \frac{2\alpha_M(\mathcal{P})\delta - \alpha_m(\mathcal{Q})}{\alpha_m(\mathcal{P})} \nu \quad (21)$$

After integration, we can finally write:

$$\nu(t) \leq \xi e^{-\lambda t} \nu(0) \quad (22)$$

where $\xi \in \mathfrak{R}$ and $\lambda = \frac{\alpha_m(\mathcal{Q}) - 2\alpha_M(\mathcal{P})\delta}{\alpha_m(\mathcal{P})}$. Thus, if the condition $\frac{\alpha_m(\mathcal{Q})}{\alpha_M(\mathcal{P})} \geq 2\delta$ is satisfied, this ensures the exponential convergence of the tracking error to zero when t tends to infinity. ■

As shown in Eq. (12), the information of the disturbances is retained in the controller to attenuate

their influences. But this control law has a poor disturbance elimination capability and it is not able to reject the lumped disturbances since they must be available, which is unrealistic for any real industrial system. In the next section, we present the design of a nonlinear DO to estimate these unavailable disturbances.

4. DO and CHADPC design

4.1. Disturbance observer

For an industrial system such as a coupled two-tank MIMO process, measuring the disturbances acting on it is very difficult. However, the disturbances observation technique provides an alternative approach. In this section, we adopt the nonlinear DO presented in [26] to estimate the slow time-varying lumped unknown disturbances $d(t)$ in the general form of the dynamic model (2). The dynamics of this DO is given as:

$$\begin{cases} \dot{z} = \hat{d} - p(h) \\ \dot{z} = -l(h)z - l(h)(p(h) + f(h) + g(h)\tilde{u}) \end{cases} \quad (23)$$

where h and \tilde{u} are state and control input for the original system (2), respectively, \hat{d} is the estimated disturbances, z is the internal state of the nonlinear observer, $p(h)$ is a nonlinear function to be designed and $l(h)$ is the observer 2×2 matrix gain which, according to Ref. [26], should be designed as:

$$l(h) = \frac{\partial p(h)}{\partial h} \quad (24)$$

In this observer, the estimation error is defined as $e_d = d - \hat{d}$. Assuming that the disturbances vary slowly compared to the observer dynamics ($\dot{d} \approx 0$), and invoking (23), (24) and (2), it can be shown that the time derivative of the estimation error can be written as follows:

$$\dot{e}_d = \dot{d} - \dot{\hat{d}} = -\dot{z} - \dot{p}(h) = -l(h)e_d \quad (25)$$

Therefore, if $l(h)$ and the associated $p(h)$ are chosen, such as Eq. (24) is exponentially stable for all $h \in \mathbb{R}^2$, the estimated $\hat{d}(t)$ approaches the real disturbance $d(t)$ exponentially [16].

To ensure the convergence of the estimation error, it is important to choose the gain $l(h)$ and its corresponding $p(h)$ appropriately. Assuming that the disturbance d in (2) is multiplied by the unit 2×2 matrix, we can choose $l(h)$ as a constant matrix such that all eigenvalues of the matrix $-l(h)$ have negative real parts. Here, the integration of $l(h)$ with respect to the coupled two-tank MIMO system state h yields $p(h) = l(h)h$. The corresponding observer gain matrix $l(h)$ is then designed in the form:

$$l(h) = \text{diag}\{l_1, l_2\} \quad (26)$$

where $l_i > 0$, $i = 1, 2$. It can be deduced that the convergence of the DO is guaranteed regardless of the process state.

4.2. Composite controller

As mentioned in Remark 2.1, external disturbances coupled with modelling errors and uncertainties can significantly affect the liquid level tracking performance. These factors can even lead to instability if their influence has not been properly accounted for in the control design. In the previous derivation of ENMPC, the lumped disturbances appear in the control law. Therefore, once the DO provides an estimate of the disturbances, the ENMPC controller can take them into account and compensate for them. Since the input matrix $g(h)$ for the coupled two-tank system is a constant matrix $g(h) = \begin{bmatrix} c_2 & 0 \\ 0 & c_2 \end{bmatrix}$, the control law using the estimated disturbances is given by:

$$\tilde{u} = - \begin{bmatrix} \frac{1}{c_2} & 0 \\ 0 & \frac{1}{c_2} \end{bmatrix} (ke_h - f(h) - \dot{r} + \hat{d}) \quad (27)$$

where the hated variable $\hat{d} = \begin{bmatrix} \hat{d}_1 & \hat{d}_2 \end{bmatrix}^T$ denotes the estimated disturbances value and the other terms are defined in (12). Finally, if we consider trimming errors in the dynamics of the coupled two-tank MIMO system, the overall CHADPC law is given as:

$$u = \tilde{u} - \hat{u} \quad (28)$$

where $\hat{u} = g(h)^{-1}\hat{d}$ is the control trim error estimated by the disturbance observer. The overall block diagram of the control-observation scheme is shown in Figure 2.

5. Experimental results and discussion

5.1. Test Bench description

The analytical results given in the previous sections are validated by an experimental setup that we have recently made (see Figure 3). It is located in the laboratory "Control systems" at British Applied College, Umm Al Quwain, UAE.

The composite controller is designed like a centralized control since the information for decision-making is from a central location which is the Real Time Windows Target (RTWT) of MATLAB software. In fact, the implementation of the observer-control scheme illustrated in Figure 4 is based on Keil μ Vision5 and MATLAB/Simulink. First, the Real-Time Workshop automatically builds a C++ source program from the Simulink Model using Keil μ Vision5 and executes it inside the STM32F10 microcontroller as the interfacing program. This is called the Target application, which ensures the interfacing role of the Input/Output Board. Then, the RTWT, acting as the host program and containing the control-observer Simulink models, communicate with the experimental apparatus via the I/O Board making a non-costly real-time control.

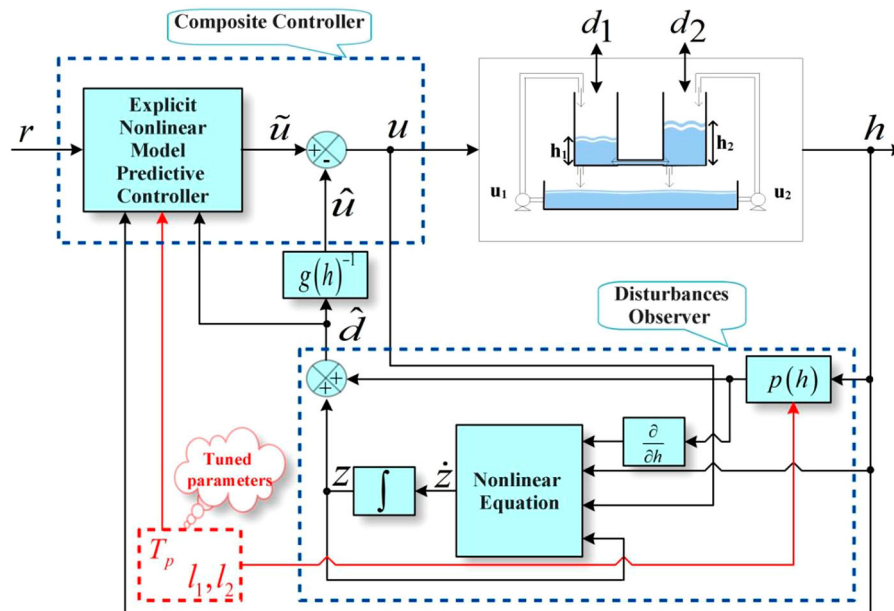


Figure 2. Conceptual diagram of the CHADPC method.

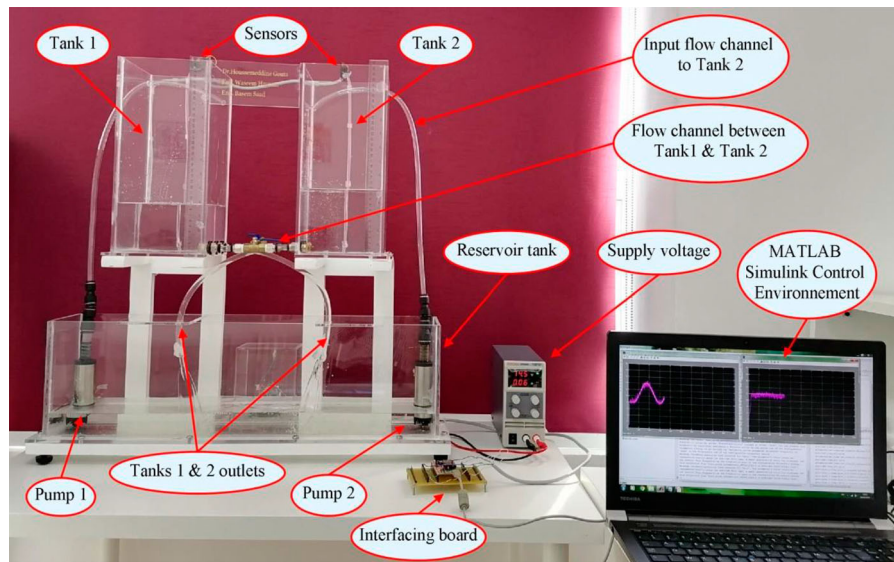


Figure 3. Experimental setup.

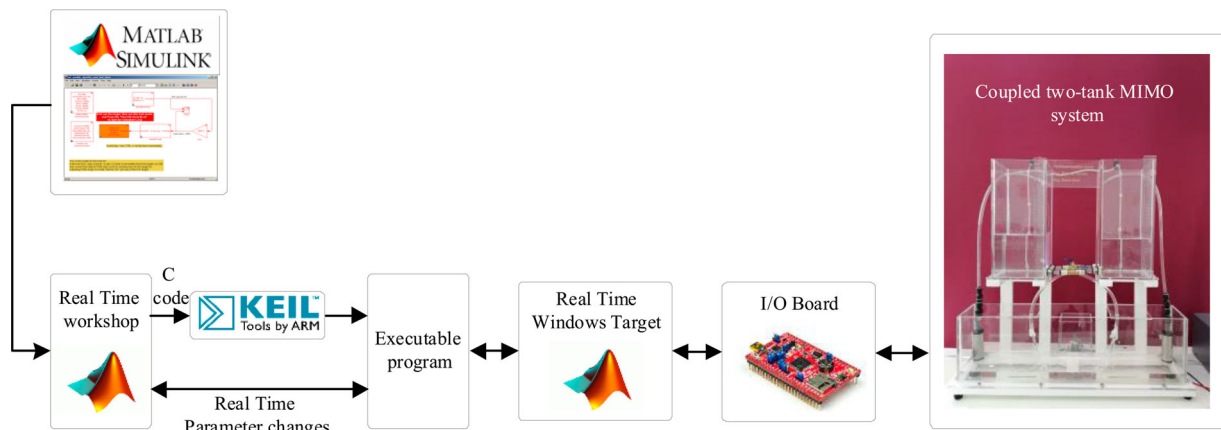
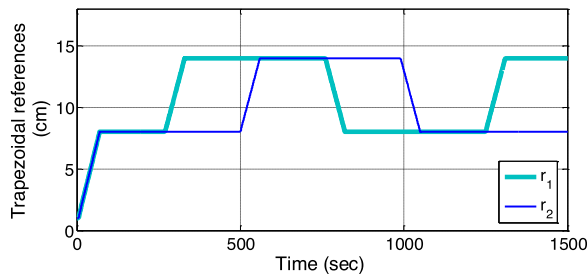


Figure 4. Control system development flow diagram.

Table 2. Numerical values of controller parameters.

Parameter	Symbol	Numerical value
Prediction horizon	T_p	0.13s
DO matrix gain	$l(h)$	$diag\{10, 10\}$

**Figure 5.** Trapezoidal benchmark references.

Before deriving the main results, the system parameters c_1 , c_2 and c_{12} shown in (1) have been calculated using the numerical values illustrated in Table 1. The designed controller-observer requires the tuning of three parameters: T_p for the ENMPC and $diag\{l_1, l_2\}$ for the DO. First, T_p has been slightly adjusted by trial and error in preliminary simulation tests without adding the DO until a good tracking performance is obtained. Then, the values of the observer design parameters l_1 and l_2 have been chosen by trial and error until the interposed DO ensures accurate observation of some applied simulation disturbances. The adopted numerical values are shown in Table 2.

The validation of the theoretical results is performed by two initial experimental tests using the closed loop benchmark consisting of a time-varying reference signal $8\mu(t-10) + \left\{3 \sin\left(\frac{2\pi(t-112.5)}{250}\right) + 3\right\} \{\mu(t-50) - \mu(t-800)\}$ and a step signal $10\mu(t)$ used as reference trajectories for h_1 and h_2 , respectively. In the presence of two external perturbations, the controller's objective is to track the two reference benchmarks well and discard the perturbations while a duration of 15min. In the first test, ENMPC is applied to the real system, while the DO is integrated and CHADPC is applied in the second test. Furthermore, CHADPC is revalidated with trapezoidal reference trajectories with large changes in different equilibrium points (see Figure 5). The sampling time is always equal to 0.01s and the selected frequency of the PWM signals applied to the actuators is 15kHz. Each liquid level is measured with the differential pressure sensor MPX5010dp. This piezoresistive transducer was chosen because it is well suited for appliance liquid levels and for microcontroller-based systems.

5.2. Experiments and discussion

In order to test the robustness of the designed controllers in the presence of lumped disturbances, the

application of the time-varying reference signal and the step signal references is accompanied by two additional external perturbations suddenly introduced on h_2 and h_1 at 500th and 700th seconds, respectively. They have been performed by pouring an additional 500cm^3 of liquid, increasing the h_1 and h_2 levels by 22% and 17%, respectively. The designed control laws (12) and (28) are first simulated in MATLAB/Simulink environment. The simulated responses of the control system via ENMPC and CHADPC approaches are shown in Figure 6. The responses show that the overshoot and the perturbation attenuation are improved with the CHADPC scheme (see the profile of the output in Figure 6(a) at 700th second and in Figure 6(b) at 500th second). Notice also that due to the interconnected DO, the CHADPC method eliminates the undesired impact of each applied perturbation in Tank i on the other liquid level h_j , $i \neq j$. In fact, Figure 6(a) shows that the perturbation on liquid level h_2 at 500th makes an undesired impact on liquid level h_1 in the case of ENMPC. This impact is totally eliminated by CHADPC method. Similarly, the impact of the second perturbation is deleted in liquid level h_2 at 700th second.

The synthesized ENMPC law (12) without integrating the DO is first experimentally tested and the results are shown in Figure 7. It can be seen that the ENMPC method maintains a good reference tracking of h_1 , while cancelling the variation in h_2 . The two perturbations are clearly attenuated in the two tanks. It can be concluded that the demonstrated exponential stability of the ENMPC law (12) is experimentally validated by the first applied experimental test.

The second experimental control test is performed by the implementation of the CHADPC law (28) following the conceptual diagram shown in Figure 2. The tracking performances of this composite controller are given in Figure 8. By comparing the expanded views in Figures 7 and 8, we can see that CHADPC performs better than ENMPC in terms of tracking performance. Note that when the noise affects the system, as in this real-time hardware experimentation, the tracking performance of ENMPC is the poorest among the two methods. We can also see by comparing the expanded views of Figures 7 and 8 that the external perturbations are more quickly rejected by the CHADPC method. Quantitative comparisons of CHADPC performances with those of ENMPC are presented in Table 3. The comparison shows that the CHADPC performs better in terms of root mean square (RMS) tracking errors and RMS controller energies. In fact, the RMS values of control signals u_1 and u_2 are respectively 4.7% and 5.1% less for CHADPC than that of ENMPC, which means CHADPC reduces the control efforts. It can be also clearly remarked from Figures 7 and 8 as well from Table 3 that the subtraction of the control trim error \hat{u} deduced from the DO enhances the control performances. The RMS tracking errors for h_1 and h_2

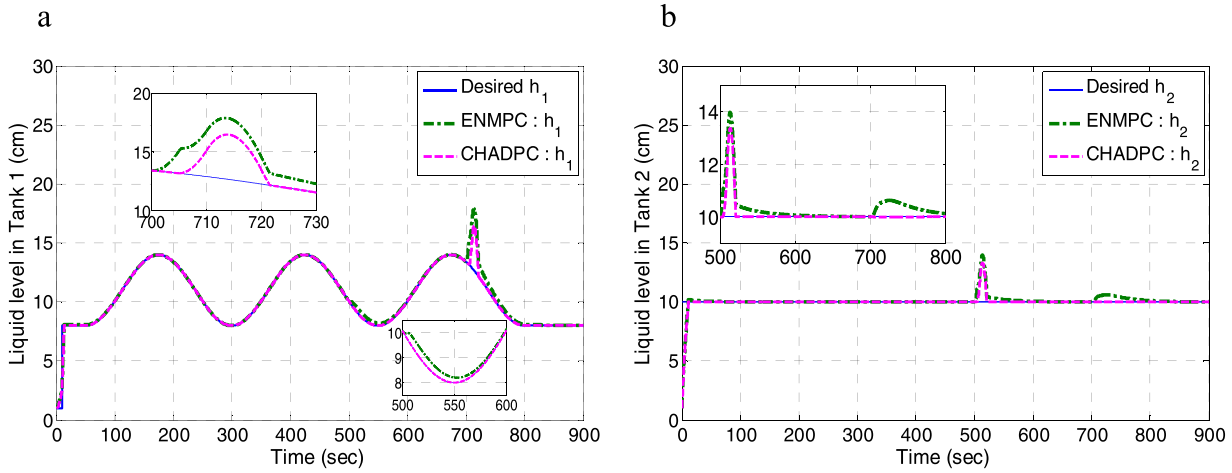


Figure 6. ENMPC and CHADPC simulated tracking performance: liquid level h_1 under perturbation at 700 sec and liquid level h_2 under perturbation at 500 sec.

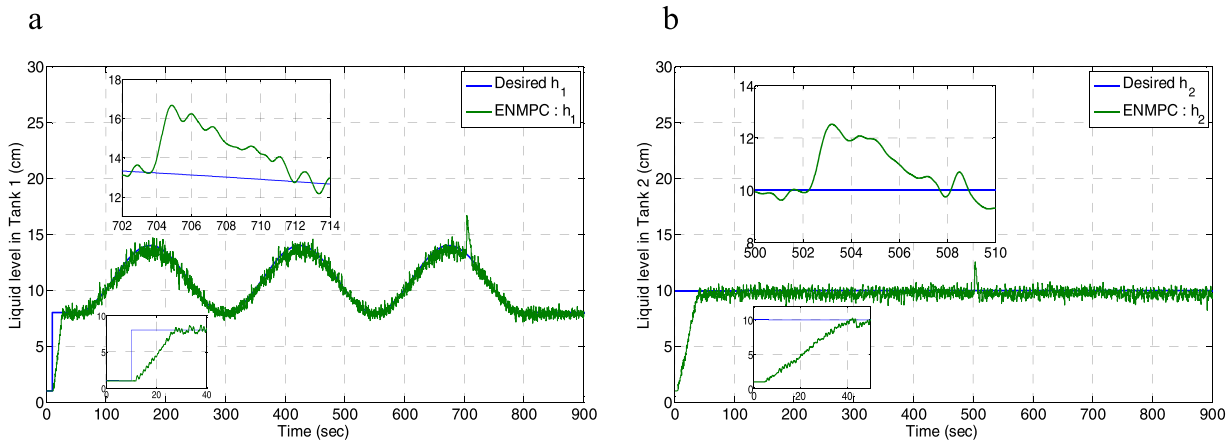


Figure 7. ENMPC tracking performance: liquid level h_1 under perturbation at 700 s and liquid level h_2 under perturbation at 500 s.

are reduced by 19.2% and 23.9%, respectively, with the CHADPC approach.

Figure 9 illustrates the control signal exerted by the two designed controllers. It can be shown that due to the variation of level h_1 , the control signal u_1 (input to Pump 1) varies periodically with the same fundamental frequency. However, the control signal u_2 (input to Pump 2) also varies periodically with the same fundamental frequency, but in opposite phase of h_1 in order

to nullify the change in h_2 due to the disturbances caused by the level h_1 . This physically means when h_1 is increasing, the ENMPC pumps less liquid to Tank 2 to minimize the variation in h_2 and vice versa. Furthermore, at 500th and 700th the control signals u_2 and u_1 , respectively, drop to 0 V so that the corresponding liquid level drops to its benchmark reference and the influence of the perturbation is thus eliminated. On the other hand, we remark from comparing the control

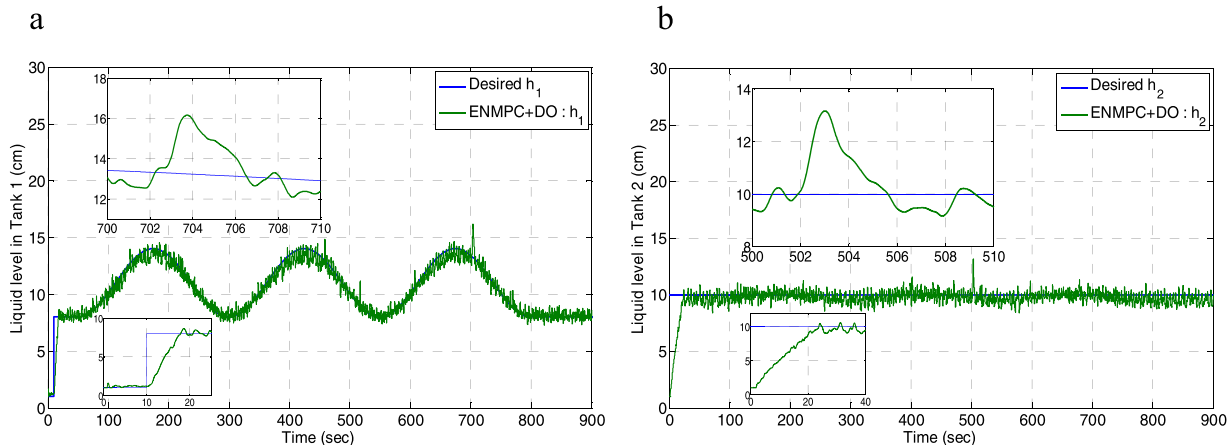
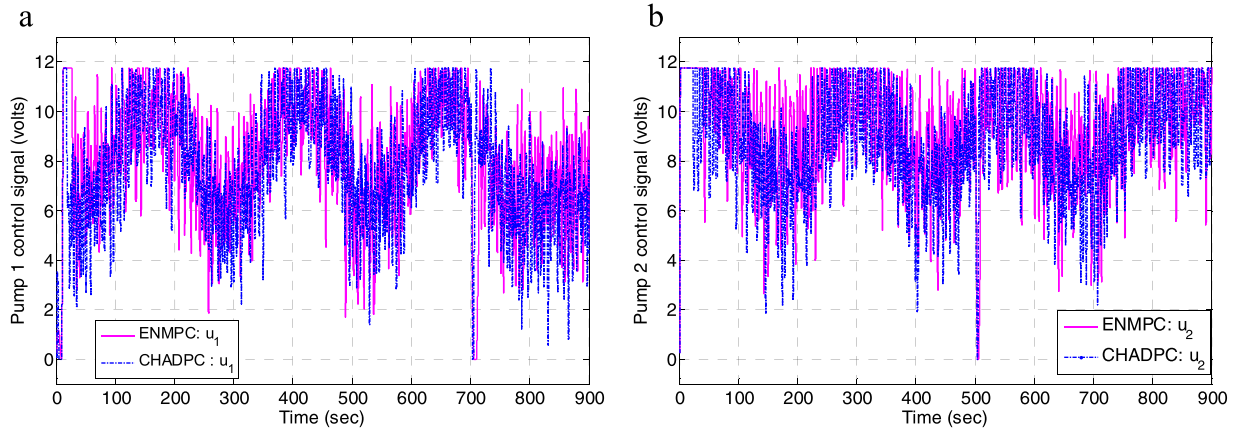


Figure 8. CHADPC tracking performance: liquid level h_1 under perturbation at 700 s and liquid level h_2 under perturbation at 500 s.

Table 3. Tests 1 and 2: summary of performances.

Control method	Liquid level in Tank 1			Liquid level in Tank 2				
	t_{s1} [s]	RMS u_1 [volt]	RMS e_1 [cm]	t_{r1} [s]	t_{s2} [s]	RMS u_2 [volt]	RMS e_2 [cm]	t_{r2} [s]
ENMPC	$\cong 25$	8.29	0.76	$\cong 8$	$\cong 41$	9.39	1.29	$\cong 6$
CHADPC	$\cong 16$	7.90	0.62	$\cong 4.5$	$\cong 24$	8.91	0.98	$\cong 3.5$

Note: t_{sj} , t_{rj} and e_j ($j = 1, 2$) are the settling time, the perturbation rejection duration and the steady state error in Tank i , respectively.

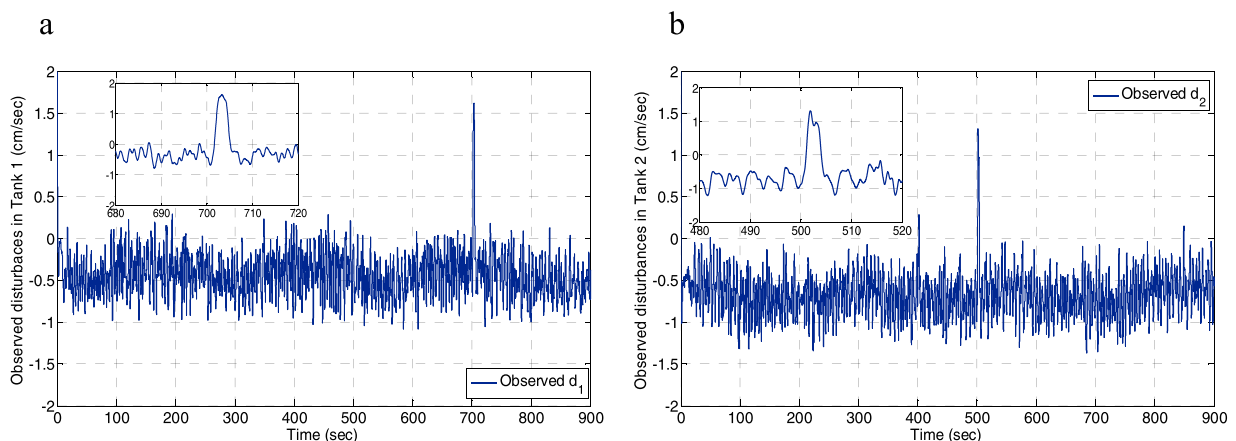
**Figure 9.** ENMPC and CHADPC methods: Pump 1 and Pump 2 control signals.

signals in Figure 9, that the CHADPC reduces the fluctuations in the control signals. This can be explained that the information given by the DO include also the level measurement noise caused by the sensors output signals. This additional small disturbance is attenuated by the CHADPC which allows more comfortable functioning to the actuators.

The disturbances \hat{d}_1 and \hat{d}_2 observed by the interconnected DO in the CHADPC method are shown in Figure 10. Without considering the two perturbations, the variation of $\hat{d}_1(t)$ varies between -1 and 0 cm/sec while the variation of $\hat{d}_2(t)$ varies between -0.5 and -1.25 cm/s. Their respective mean values are -0.4249 cm/s and -0.6673 cm/s. This is physically explained by the fact that h_1 and h_2 tend to undergo quasi-constant negative variations caused by the long distances between each pump and its corresponding tank (see Figure 3). In fact, this time delay between each

control decision and the arrival of the corresponding liquid in the tanks causes a continuous small drop of the liquid level which should be taken into consideration in the controller to enhance the tracking performance. The expanded views in Figure 10 show also the observation of the two perturbations applied at the 500th and 700th seconds as sudden increases of about 2.5 cm in each level. These observations are delivered by the DO as a sudden $+2$ cm/s variation in each tank. This quantitative analysis gives good confidence in the proposed DO.

In a third experiment, the CHADPC method is validated again. Figure 11 shows the experimental evolution of the trajectory tracking of h_1 and h_2 when the objective is to track the two trapezoidal benchmarks illustrated in Figure 5. It can be seen that the proposed control-observer design exhibits excellent decoupling performance and the tracking error is substantially

**Figure 10.** CHADPC tracking performance: Observed lumped disturbances $\hat{d}_1(t)$ and $\hat{d}_2(t)$.

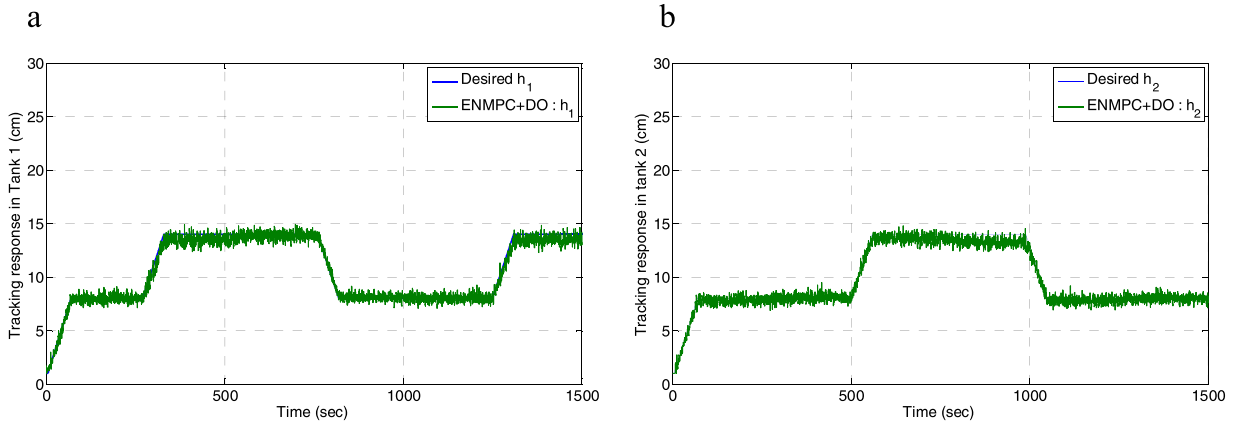


Figure 11. CHADPC method in the third experiment: tracking responses of liquid levels h_1 and h_2 .

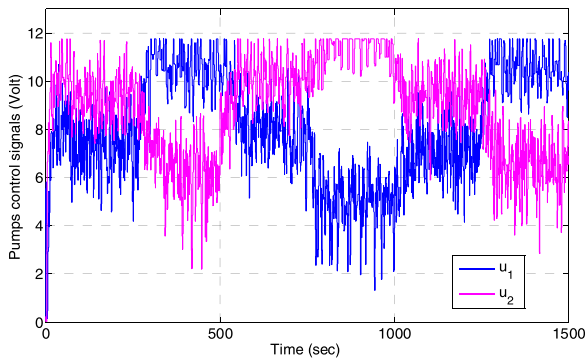


Figure 12. CHADPC method in the third experiment: Pumps 1 and 2 control signals.

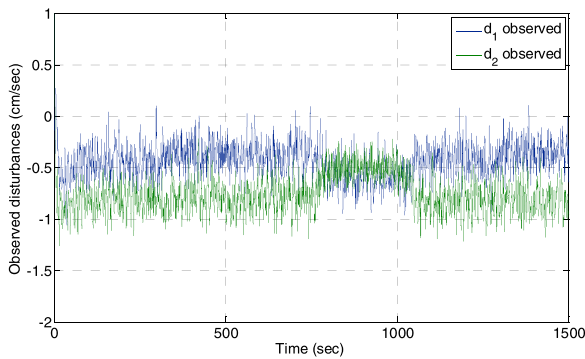


Figure 13. CHADPC method in the third experiment: Observed lumped disturbances $\hat{d}_1(t)$ and $\hat{d}_2(t)$.

reduced to a small neighbourhood of zero. Figure 12 shows the two control signals. As shown in Figure 5, we can divide the test duration into six intervals according to the comparison between the values of r_1 and r_2 . For example, in the second time interval (from the 330th to the 560th second), r_1 is increased to 14cm while r_2 remains the same as 8cm. As a result, due to the concept of hydrostatics, the composite controller pumps less liquid into Tank 2, because the liquid is also coming from Tank 1, as $h_1 > h_2$ during this interval. This can be seen in Figure 13 by the decrease of u_2 during this interval.

The disturbances \hat{d}_1 and \hat{d}_2 observed by the DO are given in Figure 13. It is shown that they remain negative

during the third experimental test, as in the previous test, due to the delay of the liquid transport from each pump to its corresponding tank. Moreover, we can remark that when the level h_i increases, the modulus of \hat{d}_i decreases due to the decrease of the distance between the corresponding liquid surface and the pump and vice versa. This phenomenon confirms the previous given explanation about the dynamics of the observed slow time-varying disturbances in the two first experimental tests.

In conclusion, from the above discussion, it can be seen that the ENMPC is able to deal with the non-measurable disturbances and compensate for the steady-state error which is mainly caused by external non-measurable disturbances. But it has small side-effects like the aggressive control. Obviously, the CHADPC technique (ENMPC method augmented by the DO) outperforms ENMPC in disturbance rejection and provides more accurate tracking by minimizing the settling times, the perturbation rejection durations and the steady-state errors (as seen in Table 3). The measurement of the disturbances by the DO provides an important new added value to the control decision in the CHADPC, which shows these enhancements in the performances. However, the CHADPC has some disadvantages. In fact, this technique requires more computation effort due to the parallel executions of the controller and the observer. Moreover, this composite controller has three parameters (T_p , l_1 and l_2) and requires more tunings than the ENMPC (with only T_p) as well as each miscalculation made by the DO may cause a tracking divergence since the online control calculation is based on the observed values of the non-measurable disturbances.

5.3. Performance comparison with recent reported works

As can be seen in model (1), the dynamics of a multi-tank system depends on the area of the tanks and the cross-sectional areas, which directly affect its

Table 4. Comparisons with recent reported literatures.

Reference benchmarks	Design methodology	RMS e_1 [cm]	RMS e_2 [cm]	Remarks
A time-varying reference signal and a step reference signal	ENMPC (This paper)	0.7688	1.2919	Easy to design and implement in real time. Provides better set-point tracking and good disturbance rejection. Reduces tracking errors compared to controllers in [4]. No need for model linearization. No need for complex on-line calculations for an optimization algorithm
	CHADPC (This paper)	0.6208	0.9821	Overlaps with all remarks of ENMPC but suppresses external disturbances faster. Reduces root mean square errors and root mean square control energy compared to ENMPC (see Table 3). Reduces noise in control signals and provides more comfort for actuators
	PI Control [4]	1.5333	1.6268	Easy to design, implement, provides good set-point tracking and disturbance rejection. However, successful implementation of any of these controllers first requires linearization of the system. Therefore, several tests should be performed first to match the real system and the linearized model. No tested perturbations rejections are applied during the control tests
	PID Control [4]	1.5975	1.7669	
	Fractional-order PI with feed forward Control [4]	1.4915	1.5926	
	Wavelet neural network-based MPC [28]	–	–	The results show slightly better performance than all the previous controllers. Promising experimental results in abnormal situations (valves malfunctions) are shown in this study. However, for a successful real-time implementation of this controller, an initial computational setup is required to compute the optimization algorithm online. Most complex design comparing with the other methods and more computation effort is needed

parameters. Moreover, the type of sensors and the maximum flow rate provided by the actuators result in different boundary conditions for different apparatus. Thus, if the experimental setup is not approximately uniform, it may not be useful to make an accurate comparison of the level control performance with other works. In the literature, we consider the works presented in [28] and [4] as the most important recent works done in the control of the studied two-tank MIMO liquid level system. In this section, we revisit these two studies, which used two apparatus for their experimental validations different from the current used experimental setup shown in Figure 3. In [28], the coupled tank apparatus TQ CE105MV is used, while the four-tank system Feedback Instruments 33-041S is used in [4]. Despite these differences, rough experimental results comparisons are given in Table 4. Since the time-varying reference signal and with the step reference signal benchmarks are close to those used in this work are used in [4], the RMS tracking errors are quantitatively compared with the three controllers presented in [4] which are the PI, PID and fractional-order PI. On the other hand, only a qualitative comparison is made with the wavelet neural network-based MPC in [28].

From the waveform of the real-time control, we can see the superiority of the designed CHADPC and a significant improvement in the tracking errors compared to all the controllers applied in [4]. However, the control method used in [28] outperforms slightly better than CHADPC, but it requires a more complex design and

much more computation efforts. Moreover, it is worth highlighting that we have obtained competitive results for the tracking performances, although the apparatuses used in [28] and [4] are much more convenient for the experiments than our locally built apparatus.

6. Conclusions

This paper describes a composite control scheme for the level tracking of a coupled two-tank MIMO system. The proposed control methodology (CHADPC) is based on the use of an overlapping implementation of a DO, in order to estimate the lumped disturbances acting on the controlled liquid levels, and on the use of an explicit solution of the nonlinear MPC. The global exponential stability of the proposed ENMPC approach has been demonstrated. The performances of the proposed ENMPC and CHADPC have been experimentally tested on a real laboratory prototype. The experiments show a high performance over the some recent designed controllers in terms of trajectory tracking tasks. The robustness and disturbance attenuation are improved by integrating the DO and designing the CHADPC method. This proposed control scheme solves the difficulties caused by the measurement noises and the mismatches in the calculated parameters in applying the model-based control in a practical environment. It also has the ability to estimate the trim conditions and give a better condition to the actuators. Finally, the presented disturbances rejection-based

control methodology is well suited to deal with complex control system problems. Due to its versatility and simple real-time implementation, the synthesized CHADPC is suitable to be robustly used in a variety of real-world engineering applications, such as the level control of the multiple-tank MIMO system.

Acknowledgments

The authors are grateful to the Administration Department of British Applied College. Also, Houssemeddine is highly grateful to Prof. Faouzi M'Sahli and Dr. Salim Hadj Saïd (from University of Monastir, Tunisia) for their support during his previous research works, prior to his Ph.D, which led to this current work.

Disclosure statement

No potential conflict of interest was reported by the authors.

Funding

This work was supported by the Administration Department of British Applied College, Umm Al Quwain, UAE.

ORCID

Houssemeddine Gouta  <http://orcid.org/0000-0003-0954-5210>

References

- [1] Alex J, Beteau J, Copp J, et al. Benchmark for evaluating control strategies in wastewater treatment plants, European Control Conference (ECC); 1999. p. 3746–3751.
- [2] Pokhrel D, Viraraghavan T. Treatment of pulp and paper mill wastewater a review. *Sci Total Environ.* 2004;333(1–3):37–58.
- [3] Kazunori U, Atsunori K, Ichiro H, et al. Automated drug delivery system to control systemic arterial pressure, cardiac output, and left heart filling pressure in acute decompensated heart failure. *J Appl Physiol.* 2006;100(4):1278–1286.
- [4] Roy P, Roy BK. Fractional order PI control applied to level control in coupled two-tank MIMO system with experimental validation. *Control Eng Pract.* 2016;48:119–135.
- [5] Hadi NH, Ibraheem IK. Speed control of an SPMSM using a tracking differentiator-PID controller scheme with a genetic algorithm. *Int J Electr Comput Eng.* 2021;11(2):1728–1741.
- [6] Ruiz JM, Giraldo JA, Duque JE, et al. Implementation of a two-tank multivariable process for control education. IX International Congress of Mechatronics Engineering and Automation (CIIMA); 2020. p. 1–6.
- [7] Gouta H, Hadj Said S, M'Sahli F. Model-based predictive and backstepping controllers for a state coupled four-tank system with bounded control inputs: A comparative study. *J Frankl Inst.* 2015;352:4864–4889.
- [8] Gouta H, Hadj Said S, Turki A, et al. Experimental sensorless control for a coupled two-tank system using high gain adaptive observer and nonlinear generalized predictive strategy. *ISA Trans.* 2019;87:187–199.
- [9] Wang G, Jia Q-S, Qiao J, et al. Deep learning-based model predictive control for continuous stirred-tank reactor system. *IEEE Trans Neural Netw Learn Syst.* 2021;32(8):3643–3652.
- [10] Heshmati-Alamdari S, Karras GC, Marantos P, et al. A robust predictive control approach for underwater robotic vehicles. *IEEE Trans Control Syst Technol.* 2020;28(6):2352–2363.
- [11] Muller C, Quevedo DE, Goodwin GC. How good is quantized model predictive control with horizon one? *IEEE Trans Autom Control.* 2011;56(11):2623–2638.
- [12] Chen W, Ballance D, Gawthrop P. Optimal control of nonlinear systems: a predictive control approach. *Automatica.* 2003;39:633–641.
- [13] Gao Z. On the centrality of disturbance rejection in automatic control. *ISA Trans.* Jul. 2014;4(53):850–857.
- [14] Guo L, Chen W-H. Disturbance attenuation and rejection for systems with nonlinearity via DOBC approach. *Int J Robust Nonlinear Control.* Feb. 2005;15(3):109–125.
- [15] Guo L, Cao S. Anti-disturbance control theory for systems with multiple disturbances: a survey. *ISA Trans.* Jul. 2014;53(4):846–849.
- [16] Chen W, Ballance D, Gawthrop PJ, et al. A nonlinear disturbance observer for robotic manipulators. *IEEE Trans Ind Electron.* 2000;47(4):932–938.
- [17] Sun W, Zhang J, Liu Z. Two-time-scale redesign for antilock braking systems of ground vehicles. *IEEE Trans Ind Electron.* 2018;66(6):4577–4586.
- [18] Brahmi B, Driscoll M, El Bojairami IK, et al. Novel adaptive impedance control for exoskeleton robot for rehabilitation using a nonlinear time-delay disturbance observer. *ISA Trans.* 2021;108:381–392.
- [19] Lai J, Yin X, Yin X, et al. Fractional order harmonic disturbance observer control for three-phase LCL-type inverter. *Control Eng Pract.* 2021;107:104697.
- [20] Ho CM, Tran DT, Ahn KK. Adaptive sliding mode control based nonlinear disturbance observer for active suspension with pneumatic spring. *J Sound Vib.* 2021;509:116241.
- [21] Abdul-Adheem WR, Ibraheem IK. Model-free active input-output feedback linearization of a single-link flexible joint manipulator: an improved ADRC approach. *Meas Control.* 2021;54:856–871.
- [22] Abdul-Adheem WR, Ibraheem IK. Decoupled control scheme for output tracking of a general industrial nonlinear MIMO system using improved active disturbance rejection scheme. *Alex Eng J.* 2019;58:1145–1156.
- [23] Najm AA, Ibraheem IK. Altitude and attitude stabilization of UAV quadrotor system using improved active disturbance rejection control. *Arab J Sci Eng.* 2020;45:1985–1999.
- [24] Roman RC, Emil Precup R, Petriu EM. EM. Hybrid data-driven fuzzy active disturbance rejection control for tower crane systems. *Eur J Control.* 2021;58:373–387.
- [25] Zhang H, Liu X, Ji H, et al. Multi-agent-based data-driven distributed adaptive cooperative control in urban traffic signal timing. *Energies.* 2019;12(7):1–19.
- [26] Chen W, Yang J, Guo L, et al. Disturbance-observer-based control and related methods – an overview. *IEEE Trans Ind Electron.* 2016;63:1083–1095.
- [27] Isidori A. *Nonlinear control systems: An introduction.* 3rd ed. New York: Springer; 1995.
- [28] Owa K, Sharma S, Sutton R. A wavelet neural network based non-linear model predictive controller for a multi-variable coupled tank system. *Int J Autom Comput.* 2015;12:156–170.